RESEARCH ARTICLE



Check for updates

Performance of an aptamer-based neuropeptide Y potentiometric sensor: dependence on spacer molecule selection

Hayley Richardson^{1,2} | Alex Kline² | Spyridon Pavlidis²

¹Department of Materials Science and Engineering, North Carolina State University, Raleigh, NC, USA

²Department of Electrical and Computer Engineering, North Carolina State University, Raleigh, NC, USA

Correspondence

Spyridon Pavlidis, Department of Electrical and Computer Engineering, North Carolina State University, Campus Box 7911, Raleigh, NC 27695-7911, USA. Email: spavlidis@ncsu.edu

Funding information

U.S. National Science Foundation (NSF), Grant/Award Number: ECCS-1936772: NSF Center for Advanced Self-Powered Systems of Integrated Sensors and Technologies (ASSIST), Grant/Award Number: EEC-116048

Abstract

Neuropeptide Y (NPY) plays a central role in a variety of emotional and physiological functions in humans, such as forming a part of the body's response to stress and anxiety. This work compares the impact of MCH and PEG spacer molecules on the performance of a potentiometric NPY sensor. An NPY-specific DNA aptamer with thiol termination was immobilized onto a gold electrode surface. The performance of the sensor is compared when either an MCH- or PEG-based self-assembled monolayer is formed following aptamer immobilization. Backfilling the surface with alkanethiol spacer molecules like these is key for proper conformational folding of aptamer-target binding. Non-specific adhesion of NPY to the MCH-based sensor surface was observed via surface plasmon resonance (SPR), and then confirmed via potentiometry. It is then shown that PEG improves the sensor's sensitivity to NPY compared to the surfaces with an MCH-based SAM. We achieve the detection of picomolar range NPY levels in buffer with a sensitivity of 36.1 mV/ decade for the aptamer and PEG-based sensor surface, thus demonstrating the promise of potentiometric sensing of NPY for future wearable deployment. The sensor's selectivity was also studied via exposure to cortisol, a different stress marker, resulting in a 13x smaller differential voltage (aptamerspecific) response compared to that of NPY.

KEYWORDS

aptasensor, neuropeptide Y, potentiometry, spacer molecule, surface plasmon resonance

INTRODUCTION 1

Personalized healthcare is projected to increase with growing demand for point-of-care detection and realtime results [1]. With the rising cost of health services, tailoring medicine to individuals' needs is becoming more vital to save patients' time and money. The lowpower consumption of synthetic affinity biosensors makes them marketable to many communities. When employed, self-assembled monolayers (SAM) that aid in the generation of an interpretable electrical signal from a

biological medium are a crucial biorecognition element in electrochemical sensing. The quality of the SAM is directly related to the parameters and environment selected during the assembly procedure. The processing and performance relationships for a specific SAM are difficult to estimate without experimentation that examines the interdependencies of the molecular biophysics, electrolyte composition, and surface formation.

Neuropeptide Y (NPY) is a peptide found abundantly in the human nervous system. Concentration levels of NPY can connote how intensely a body responds to

stress and the time it takes to re-equilibrate to homeostatic levels [2]. Elevated basal levels of NPY have been linked to depressive disorders, traumatic events, and military operational stress [3,4]. For example, it has been reported that the NPY concentration in sweat can spike nearly 90 times as high in people with depression than the range for people without depression (3.34–17.21 pM compared to 0.19–0.21 pM) [5]. A novel wearable biosensor that could continuously monitor NPY concentrations would therefore stand to play an important role in supporting mental health, as well as individuals with high-stress occupations. This sensor would furthermore introduce a quantifiable metric to improve diagnosis procedures and help individuals identify their specific stress triggers in real time.

Because of the physiological importance of NPY, many other groups have recently investigated detection with varied approaches. Mendonsa et al. used capillary electrophoresis-systematic evolution of ligands by exponential enrichment (CE-SELEX) to discover an 80base ssDNA aptamer that selectively binds to human NPY [6]. Aptamers as probes in electrochemical sensors have several advantages over conventional affinity biosensors that use ligands such as antibodies, like smaller size, comparable or better binding affinity, and easier chemical modifications [7]. The feasibility of this aptamer sequence as an immobilized biorecognition agent for sensors has been proven in other published research. Using gold planar electrodes, a wearable, impedancebased platform was developed to detect NPY via electrochemical impedance spectroscopy (EIS) in sweat. The correlation in cortisol and NPY levels was explored and a lowest NPY concentration of 1 pg/mL (0.2 pM) was detected in human participants, with comparable sensitivity to that of an anti-NPY antibody [8,9]. Elsewhere, NPY detection was accomplished via differential pulse voltammetry (DPV) using graphene and gold nanoparticles with the aforementioned DNA aptamer sequence co-immobilized with 6-mercapto-1-hexanol (MCH) [10]. A physiologically relevant limit of detection (LOD) of 10 pM was achieved. Graphene field-effect transistors (GFETs) have also been developed to detect NPY with a peptide recognition element (P1N3) [11], achieving a sensitivity of −13.8 mV/dec from picomolar to micromolar concentrations. We have demonstrated picomolar-level detection via cyclic voltammetry and electrochemical impedance spectroscopy on flexible gold films for use in subcutaneous sensing [12]. The NPY response in PBS was measured as low as 400 pM and showed significant differences between the aptamer-sensor when compared to a control surface of poly(ethylene glycol) methyl ether thiol (PEG)-based SAM.

In this work, we have studied the impact of surface preparation, specifically the role of the SAM spacer molecule (PEG vs. MCH), on the sensitivity and selectivity of a gold electrode-based potentiometric sensor for NPY. When sensing, the use of spacer molecules can ensure that the measured signal predominantly comes from the binding of the aptamer and the target, and not from other species such as the gold surface or within the biological medium. If spacers are not used and the surface density of the aptamer is too high, there can be a dramatic signal loss because the proper conformational folding cannot be achieved because the many nitrogen groups in the DNA backbone weakly adsorb to the surface or because of physical space restrictions between aptamers [13]. However, excess spacer molecules with polar moieties may increase the amount of non-specific interactions because of possible charge-based attraction [14]. Literature in this space has compared other molecules such as ethylene glycol thiols of different chain structures, length. zwitterionic 16-Mercaptohexadecanoic acid (MHDA), bovine serum albumin (BSA), and other antifouling materials to passivate sensors [15, 16].

For some DNA aptamer sensors, MCH has been directly compared to other oligoethylene glycol-based spacer molecules and has shown greater signal stability and response [17]. Its small carbon-chain has internal hydrophobicity while its terminal polar group may increase non-specific attraction of NPY [18]. When MCH is backfilled onto the gold sensor surface, it should not prevent the aptamer from properly conforming when bound to NPY; however, the possibility of large packing density and monolayer disorder may cause significant unwanted interactions between MCH and NPY [19]. On the other hand, the chemical structure of the 2 kDa molecular weight PEG has advantages like a non-polar head group that is exposed to the bulk solution and diffusing NPY. Its chain length is smaller than the thiolated DNA aptamer used here, which prevents the formation of polymer brushes and related non-specific adhesion [20].

In previous work, our group has investigated the potentiometry response of an RNA aptamer-functionalized electrodes for the detection of histone proteins [21]. There, we directly compared the response of increasing calf thymus histone (CTH) on a bare gold surface, MCH-only SAM, and PEG-only SAM. PEG-only SAM results showed the lowest change in voltage and was used in further aptamer-based sensing. Thus, in this test bench, there is preceding data that suggests PEG spacers are ideal for RNA aptamer-based sensors when detecting proteins. Here, we provide an in-depth systematic study of PEG- and MCH-based co-SAMS for aptamer-based NPY detection to determine whether oligoethylene

glycol-based spacers once again provide superior performance.

Thus, we report on the sensitivity and specificity achieved for MCH- and PEG-based SAMs in combination with a NPY-specific DNA aptamer recognition element [6]. The sensors are developed on gold thin film electrodes, which are easily deployable on a wide range of substrates. Preliminary validation through surface plasmon resonance (SPR) showed that MCH was a non-ideal spacer due to its interaction with non-specific charged moieties. Potentiometry confirmed that PEG was a more appropriate spacer molecule by its larger surface potential changes, heightened sensitivity to NPY in solution, and selectivity.

2 | MATERIAL & METHODS

2.1 | Materials

The 80-base ssDNA aptamer sequence 5'-Thiol-MC6-S-S-AGCAGCACAGAGGTCAGATGCAAACCA-CAGCCTGAGTGGTTAGCGTATGTCATTTACGGACC-TATGCGTGCTACCGTGAA-3' [6] and a buffer containing 10 mM tris(hydroxymethyl)aminomethane (Tris) and 0.1 mM ethylenediaminetetraacetic acid (EDTA) were purchased from Integrated DNA Technologies Inc. (Iowa, USA). Tris[2-carboxyethyl] phosphine (TCEP) was added to the aptamer solution to reduce the disulfide bond formation. TCEP, 6-mercapto-1-hexanol (MCH), poly(ethylene glycol) methyl ether thiol (PEG), bovine serum albumin (BSA), cortisol, and cleaning detergent RNAseZapTM were all purchased from MilliporeSigma (Missouri, USA).

NPY was procured from GenScript Biotech Corp. (New Jersey, USA). NPY was dissolved in 1 or 10 mM phosphate buffer saline (PBS) (7.5 mM $\rm Na_2HPO_4$, 2.5 mM $\rm NaH_2PO_4$, 2.7 mM KCl and 137 mM NaCl) at pH 7.4 that was purchased from Cytiva (Massachusetts, USA). Gold working electrodes and the microfluidic platform were purchased from MicruX Technologies (Spain). Flow-thru reference electrodes were purchased from Microelectrodes Inc. (New Hampshire, USA).

2.2 | Electrode functionalization

To tether the aptamer to the gold electrodes, there was a thiol modification added to the 5' sequence end. The spontaneous organization of alkanethiol monolayers on gold has been well studied for sensing and thin-film applications [22]. The sulfur atoms in the thiol (-SH) deprotonate to occupy the fcc hollow sites in the (111)

plane and covalently bond with gold atoms [23]. Using a thiol modification has benefits over other types of sensor surface fabrication because it ensures that the molecule and the binding reaction are close to the electrode. This is paramount since the net electrostatic effect of the molecules' binding interaction only persists as far as is dictated by the Debye length (λ_D) [24].

Each SAM was formed in ambient conditions. Electrodes were cleaned with ethanol then submersed in $1 \mu M$ aptamer solution overnight. Then, the electrodes were rinsed with DI water, dried under N_2 , and incubated with $1 \ mM$ of MCH or PEG in Tris-EDTA buffer for three hours. Testing was performed immediately after completing the functionalization process.

2.3 | Surface plasmon resonance

SPR gold sensor chips were purchased from Cytiva. The DNA aptamer was immobilized in the SPR instrument on gold sensor surfaces in a Biacore 3000 instrument. For 15 h at 1 $\mu L/\text{min}$, 1 μM aptamer solution was flowed on one of the flow cells, *i.e.* the active cell. To backfill the active cell and to create a separate control cell, 1 mM MCH was flowed over both cells for five hours at 1 $\mu L/\text{min}$. NPY and BSA dilutions from 10 nM–3 μM were made in PBS. The binding titration results were measured with a 180 second association injection at 30 $\mu L/\text{min}$. After an analyte injection, a 600 second dissociation phase with PBS, regeneration with 50 mM NaOH and 1 M NaCl, and baseline stabilization with PBS were done before injecting the next concentration.

2.4 | Potentiometry

Potentiometric tests were performed with a Keysight B2901 A Series Precision Source/Measure Unit and controlled with a custom LabVIEW interface. The open circuit potential, indicated as Vout in Figure 1, was measured at the working electrode (WE) with respect to the reference electrode (RE). Flow rates were controlled with a syringe pump system. Before testing, new tubing was connected to the microfluidic system, the reference electrode, and the syringe pump. The system was cleaned with detergent, IPA, and DI water. PBS was flown through the system at 0.5 mL/min, then flow was stopped so the buffer could interact with the electrodes for 10 min. After this time, the voltage was recorded for six minutes prior to injecting the next solution. The first 10 min were intended to stabilize the voltage reading and the last six minutes were recorded and averaged for every concentration. This resolution is plotted as one

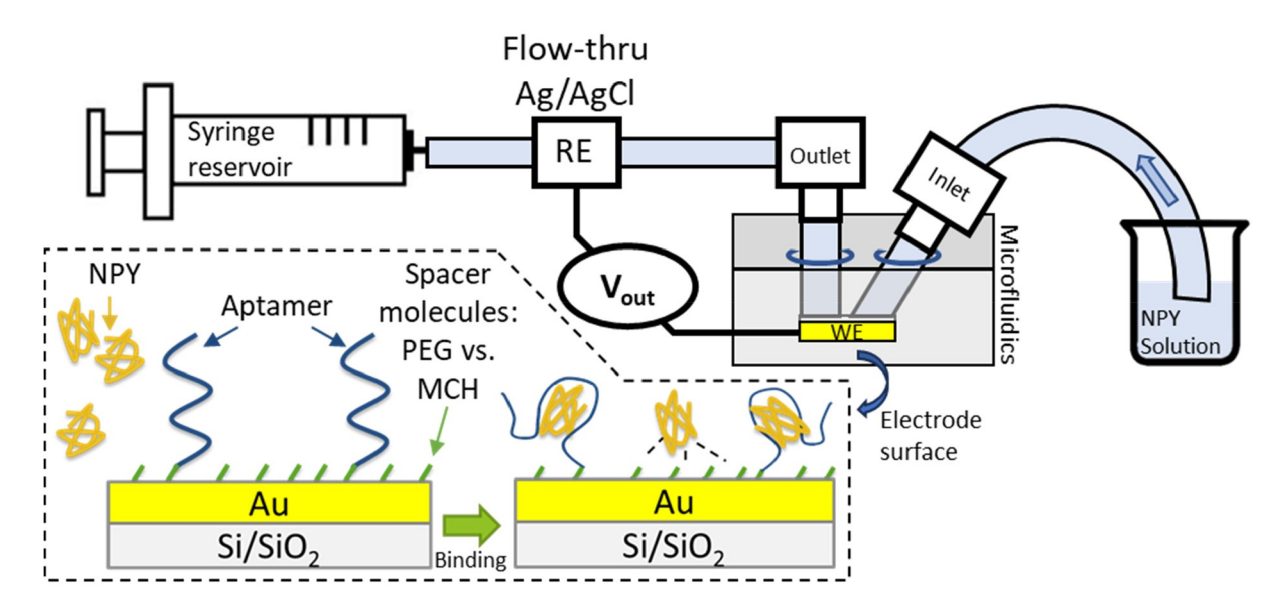


FIGURE 1 Schematic of potentiometric test bench. Fluid was drawn through tubing to flow over the working electrode that was housed in the microfluidic platform, then to the flow-thru Ag/AgCl reference electrode. Waste was collected in a syringe that was being withdrawn via syringe pump. The functionalized surface is highlighted here to show the SAM before and after binding events. Non-specific adhesion to the spacer molecule is represented with dashed lines.

standard deviation in the error bars in the potentiometric results (Figures 3, 4, 5). This was done continuously from lowest to highest concentration in a two-fold dilution series of NPY (195 pM–12.5 nM).

3 | RESULTS AND DISCUSSION

3.1 | SPR analysis of non-specific adhesion to MCH-based SAM

SPR investigated how well immobilized molecules can detect solution-phase analytes at precisely controlled flow rates. The measured response is not sensitive to any non-specific ionic interactions since SPR is an optical technique, not an electrical one [25]. The magnitude of the change in the angle of reflected light is directly proportional to the mass of material immobilized [26]. Figure 2a shows eight NPY injections over the functionalized surface with the MCH-based SAM and the curve morphology for the 180 second association injection. The curves had the baseline response value before injection subtracted and all the curves were fit to time = 0 for the beginning of the injection. The shape of the 0 µM curve was attributed to any changes in pressure when switching microfluidics on the cells and instrument drift in the dissociation baseline.

The maximum observed response at the end of the sample injection was representative of the binding amount. Peak Response Units (RUs) are plotted for NPY and BSA in Figure 2B on a semi-logarithmic scale for

concentrations 0.01 µM to 3 µM. NPY showed a strong response increase with increasing concentration injections, whereas BSA showed no correlation. When the NPY curves were fit with a single-site binding model (SigmaPlot), the extracted equilibrium dissociation constant, K_D value, was 0.36 µM, which is in agreement within the reported K_D value obtained from SELEX experiments by Mendonsa et al. [6]. BSA was used as the control orthogonal target because of its large charge density and because of the abundance of human albumin that exists in biofluid [26,27]. Although there was weak concentration dependent correlation, the measured SPR response to BSA injections was not negligible overall and corresponds to considerable non-specific adhesion of BSA. We therefore hypothesize that MCH may also electrostatically attract NPY and limit the aptamers from specifically binding, as depicted by the dashed lines in Figure 1. In the next sections, this hypothesis is tested with potentiometric measurements using electrodes prepared with different SAMs.

3.2 | Potentiometric measurements with MCH-based SAM

To investigate the behavior of the MCH-based SAM for potentiometric sensing, two separate electrodes were prepared: one was incubated with aptamer solution and then MCH (active), and the other was only exposed to MCH (control). Both functionalized electrodes were exposed to the same series of NPY dilutions. The

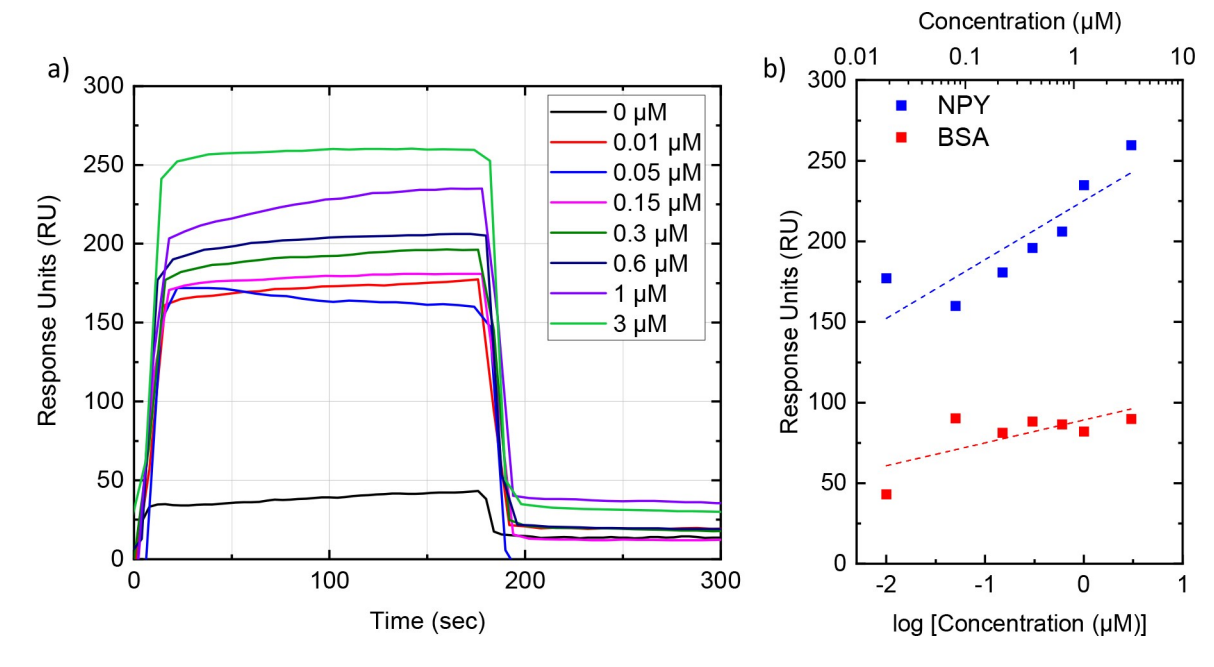


FIGURE 2 (a) Buffer-subtracted sensorgram of eight NPY concentrations on a functionalized surface with NPY-specific aptamer and MCH. (b) Semi-logarithmic comparison of peak RU value for NPY and BSA fit with logarithmic trendlines ($R_{NPY}^2 = 0.760$, $R_{BSA}^2 = 0.500$).

potentiometric response at each concentration was obtained similarly to the SPR experiments, where the initial voltage value of the buffer-only solution was subtracted from the concentration-dependent NPY solution. To calculate the voltage response attributable to the aptamer, the control surface's response was subtracted from that of the active surface. To calculate the error bars for the "Aptamer Response," the square root of the variance was calculated between the two measured data sets to achieve a useful standard deviation for each concentration. This approach also serves to minimize the impact of sensor drift, which can arise from the build-up of ions on the surface throughout the course of the continuous measurement. It is assumed that this drift was comparable regardless of the chemistry of the electrode surface; therefore, subtracting the voltage responses of the affinity SAM from the control SAM was an appropriate method of data processing.

The peak voltage values at the end of the measurement window were recorded, baseline-subtracted, and plotted in Figure 3, along with logarithmic trendline fits to assist the analysis. Both surfaces exhibited a concentration-dependent response, but the magnitude of the active surface's potential change was larger. Nonetheless, the resulting aptamer-only response for MCH had no correlation when fit with a logarithmic trendline (R² = 0.060), indicating that the differential voltage values did not trend with concentration. This is attributed to the significant degree of non-specific adhesion to MCH, and is therefore in agreement with the conclusions drawn from the SPR data. In the active surface, MCH

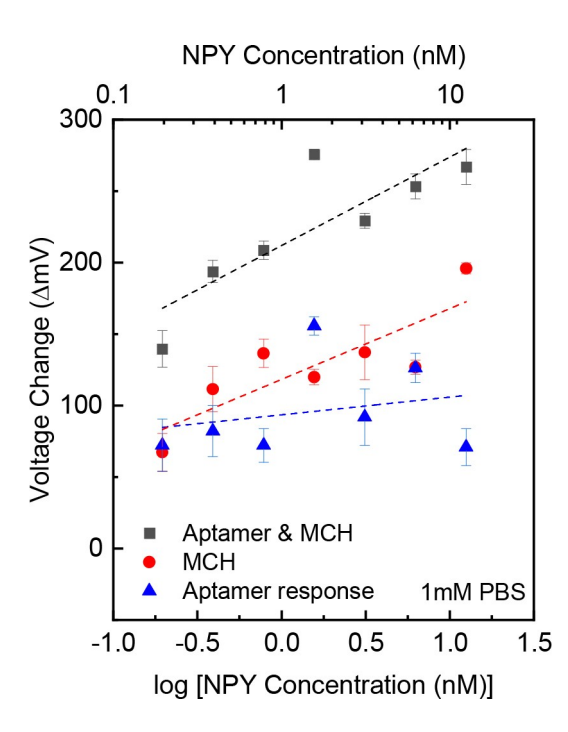


FIGURE 3 Calculated peak voltage for electrodes with an aptamer and MCH surface (black), with an MCH only surface (red), and the subtracted aptamer response (blue). Data were fit with a logarithmic trendline.

insufficiently aided the aptamer to specifically bind to NPY.

3.3 | Potentiometric measurements with PEG-based SAM

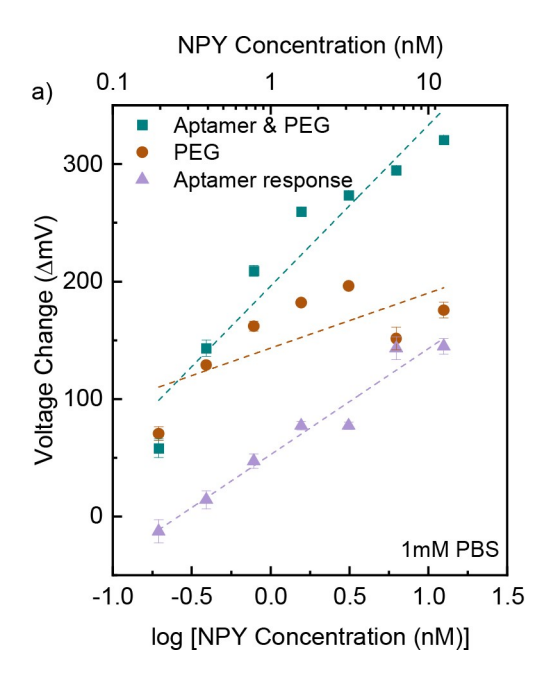
To address the shortcomings of the MCH-based SAM associated with non-specific adhesion, PEG was considered as an alternative spacer molecule. For direct comparison with the performance of the MCH-based SAM, initial measurements were done with 1 mM PBS buffer. Via comparison of Figures 3 and 4a, it can be seen that the MCH-only and PEG-only control surfaces performed similarly in both magnitude and sensitivity to NPY. The difference in the performance between the two spacer molecules was found in the mixed co-monolayer response. Figure 4a demonstrates how the active surface, formed with aptamer and backfilled with PEG, exhibited a larger response to the highest NPY concentration than the equivalent MCH-based electrode. Importantly, this resulted in a clear NPY-dependent aptamer-only response with a tighter fit to the logarithmic trendline $(R^2=0.960)$ and improved sensitivity. This indicates that PEG allowed the aptamers to capture NPY to a greater degree, thus producing larger charge transfer through the electrode.

Due to the Debye length's dependence on ionic strength, it is expected that a larger potentiometric sensor response can be obtained using diluted buffer solutions, such as the 1 mM PBS solutions employed heretofore [28]. However, buffer dilution complicates sensor deployment in the field. Thus, additional sensing tests using the PEG-based SAM were conducted in 10 mM PBS buffer, as shown in Figure 4b. Comparing Figure 4a and b, it can be seen that the electrodes in low ionic

strength buffer had larger voltage change values for both the active (green) and control (orange) surface compared to the electrodes tested in the higher ionic strength buffer. Additionally, the differential signal, corresponding to the aptamer response, demonstrated higher sensitivity to NPY in low ionic strength, as given by the slope of the logarithmic trendline, thus confirming the Debye length dependency. Ions in the high strength buffer may have migrated close to the electrode surface, but not within the Debye length screening and prevented NPY from being captured, therefore reducing the amount of binding for both the active and control surfaces. The added water content in the low strength buffer may have caused additional capacitive effects, which could make the voltage higher. Other theories indicate that the salts or inherent pH modification could affect the mass transport of NPY to the electrode surface. Although the sensor's NPY sensitivity was reduced in more complex medium, the magnitude of the aptamer contribution to the voltage signal was higher and still easily capable of being calibrated.

3.4 | PEG surface with negative control proteins

To investigate any non-specific binding from the charge interaction between different biomolecules with the aptamer or spacer, a negative control analyte of cortisol was tested. The response generated from these interactions can give insight to the magnitude of the selectivity of the desired response. The hormone cortisol was selected because of its similar water-solubility to NPY and its small molecular



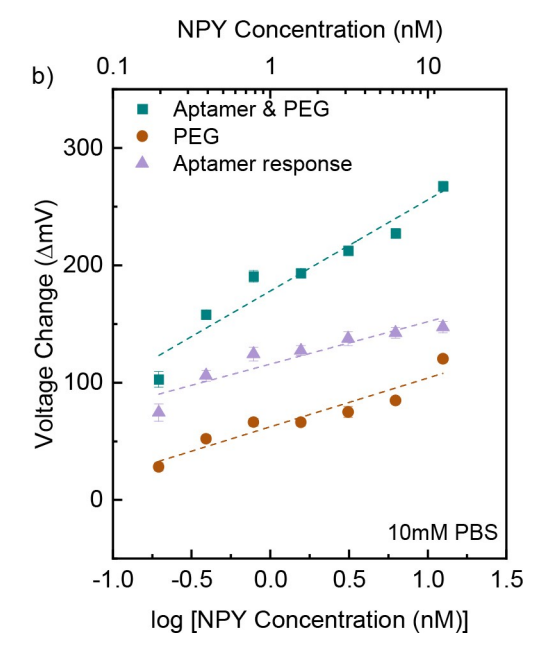


FIGURE 4 Peak voltage differentials for NPY in low (a) and high (b) ionic strength PBS buffer.

weight. Similar to NPY, cortisol is a relevant biomarker for stress monitoring. The concentration of free cortisol in sweat exists in the nanomolar range and its ability to bind to cortisol-selective aptamers have been shown in literature [29,30].

The potentiometric response of the PEG-based SAM to cortisol in 10 mM PBS is shown in Figure 5. The PEG only control electrode demonstrated a very similar sensitivity to both NPY (Figure 4b) and cortisol in 10 mM PBS. This comparison alone was insufficient to conclude that PEG was an appropriate spacer molecule for this aptamer system. There must be significant difference between the differential signals that represent the contributions of the NPY-specific aptamers themselves. While there was some cortisol interaction with both the active and control

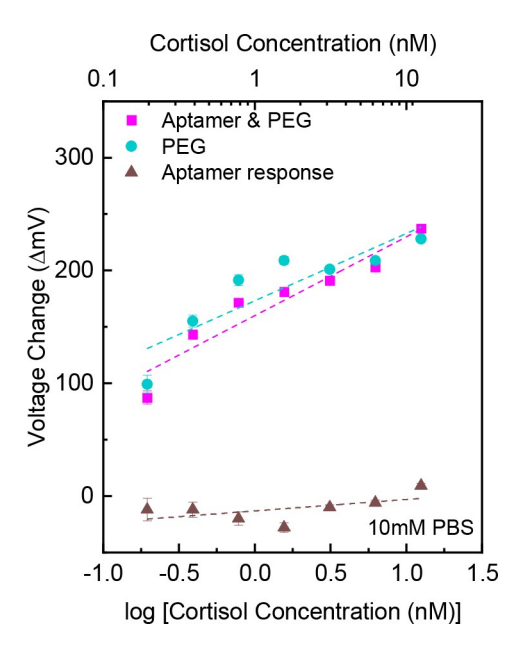


FIGURE 5 Peak voltage differentials for cortisol in high ionic strength PBS buffer.

electrodes, ultimately, the aptamer response was low, and confirms selectivity of the sensor. Because the active and control surface had nearly identical response, the sensitivity and the voltage values of the active surface with cortisol are significantly lower than that of the NPY experiment. This result was only discoverable by performing control surface experiments and analyzing the differential response.

3.5 | Comparison of results

Table 1 compares all of the systems tested for the maximum voltage change at the highest NPY concentration of 12.5 nM for the aptamer-only response, the percent contribution that the aptamer-only response had for the active surface at 12.5 nM, the strength of the correlation based on the R² statistical regression model, and the detection sensitivity from the fitted logarithmic trendline.

The voltage change calculation was dependent on the voltage recorded on the initial buffer measurement. The surfaces with MCH and the surfaces with PEG all responded to the buffer measurement based on how charges are distributed in the monolayer, regardless of the analyte that follows. Each monolayer's response to the buffer was therefore expressed within the successive measurements. Comparing this metric, the PEG surfaces in high ionic buffer measured the largest \triangle mV signal (147.3 \pm 4.9 mV). The value was over 13x that of the signal measured for cortisol when using the same surface and buffer types (9.2 \pm 2.2 mV)

The control surface likely had a higher surface density of spacer molecules compared to the active surfaces because the molecules had more available sites to immobilize to without the presence of the aptamer; hence, the voltage response may be larger than the actual non-specific binding contribution of the spacer molecule on the active

TABLE 1 Quantitative comparison across all four electrodes tested. This considered the subtracted aptamer response data, which was the contribution of the aptamer in the active surface.

Spacer	МСН	PEG	PEG	PEG
Ionic strength	1 mM	1 mM	10 mM	10 mM
Analyte	NPY	NPY	NPY	Cortisol
Aptamer voltage change (△mV)	71.0 ± 12.8	144.9 ± 6.8	147.3 ± 4.9	9.2 ± 2.2
Aptamer voltage contribution (%)	26.6 ± 17.8	45.2 ± 6.8	55.1 ± 6.3	3.9 ± 3.0
Sensitivity (mV/dec)	12.4	90.2	36.1	10.2
\mathbb{R}^2	0.060	0.960	0.862	0.328

surface. Taking this discrepancy into account, voltage contribution as a percent was also calculated. This was calculated by dividing the voltage change of subtracted aptamer response by the voltage change of active surface. The PEG system for NPY detection in high ionic strength buffer had both the higher voltage change value and percent of aptamer-only response $(55.1 \pm 6.3\%)$.

Considering the R² value, there was a statistical correlation in the data for two PEG surfaces: low ionic strength buffer with NPY (R²=0.960) and high ionic strength buffer with NPY ($R^2 = 0.862$). This may suggest that when PEG was used, the analyte-aptamer complex was stable during the injected concentration changes. Sensitivity was calculated by multiplying the slope of the logarithmic trendline with log₁₀ to achieve the mV change per decade change of concentration. The electrode used with cortisol was below the sensitivity of the PEG electrodes used to detect NPY (10.2 mV/dec vs. 36.1 mV/dec) in high ionic strength buffer. The largest sensitivity produced was for the PEG electrodes in low ionic strength buffer at 90.2 mV/dec. Additional studies will be done to further characterize the charge based, non-specific negative control interactions and how they may obscure accurate electrochemical response of the affinity sensor.

The performance of our PEG-based potentiometric NPY sensor is compared in Table 2 against other published NPY sensors using the same aptamer recognition element. At this time, our adoption of PEG as a spacer molecule to improve sensor performance represents a unique choice. As

discussed above, understanding sensor performance called for the evaluation of spacer molecule-only control surfaces without the aptamer present. The investigation of the performance of a control surface to ensure a true binding system has not been performed in other aptamer-based NPY sensor reports, but has been done for peptide-based biorecognition elements [11]. Due to its relevance to stress monitoring, cortisol has also been used in other studies as a control analyte. Our lowest NPY concentration tested falls near physiological-levels and is an improvement on earlier published results from our group [12]. While other publications have investigated lower NPY concentrations and, in some cases used complex media such as artificial sweat, we achieve the lowest detected NPY concentration using a potentiometric approach [33,34]. Future work will build on these results by improving performance and investigating deployment of our sensor in physiological solutions.

4 | CONCLUSIONS

We have demonstrated an aptamer-based potentiometric sensor with pM-level sensitivity and selectivity towards NPY, an important marker for stress and stress response. This was achieved by investigating the sensor's performance as a function of the MCH and PEG spacer molecules. Control surfaces all interacted similarly with NPY or cortisol, but the aptamer's ability to specifically interact with

TABLE 2 Comparison of sensor performance with published reports of electrochemical NPY sensors.

Transduction method	Sensor electrode	Spacer molecule	Medium	Lowest conc.	Control analyte	Ref.
Potentiometric	Gold	PEG	PBS	195 pM	Cortisol	This work
EIS	Gold	N/A	Art. sweat	1 pg/mL	Cortisol, steroid mix	[9]
EIS	Gold	PEG	PBS	400 pM	N/A	[12]
EIS	Carbon fiber/ platinum	Thioglycolic acid	Art. cere- bro. fluid	10 ng/ mL	N/A	[31]
Colorimetric	AuNP	N/A	Art. sweat	100 nM	Orexin A, BSA	[32]
FET	CNT	N/A	Serum	500 pM	Cortisol, DHEAS	[33]
DPV	Graphene- gold composite	МСН	Serum	10 pM	Orexin A, HSA, Cortisol	[10]
FET	Si NW	Propyl trimethoxy silane	PBS	10 nM	Dopamine	[34]

NPY greatly depended on which spacer molecule was adopted for SAM formation. It was found that PEG is a more effective spacer molecule than MCH: the isolated sensitivity of the aptamers is 36.1 mV/dec in 10 mM PBS when using PEG, compared to 12.4 mV/dec when using MCH in 1 mM PBS. In PEG-based tests, a discernable signal was observed for the lowest tested NPY concentration of 195 pM, and yielded a 13x smaller signal in the presence of cortisol versus NPY. Future work will focus on determining the limit of detection, further mitigating competitive binding from negative control molecules in high ionic content, and considering different spacer or preblocking molecules. These parameters will be studied to prepare the potentiometric platform for operation as a sweat sensor.

ACKNOWLEDGEMENTS

The authors are grateful for the SPR expertise of Dr. Peter Thompson, Ph.D, at the Molecular Education, Technology and Research Innovation Center (METRIC) at North Carolina State University. This work was supported by the U.S. National Science Foundation (NSF) via grant ECCS-1936772 and the NSF Center for Advanced Self-Powered Systems of Integrated Sensors and Technologies (ASSIST) supported by grant EEC-116048). Partial support was also received from NC State University Faculty Start-up funds.

CONFLICT OF INTERESTS STATEMENT

The authors declare that they have no known competing financial interests or personal relationships that could have appeared to influence the work reported in this paper.

DATA AVAILABILITY STATEMENT

The data that support the findings of this study are available from the corresponding author upon reasonable request.

ORCID

Hayley Richardson http://orcid.org/0009-0007-4898-7536

Spyridon Pavlidis http://orcid.org/0000-0002-1690-2581

REFERENCES

- A. Chaudhuri, P. Lillrank, J. Adv. Manag. Res. 2013, 10, 176– 191.
- 2. F. Reichmann, P. Holzer, Neuropeptides 2016, 55, 99-109.
- 3. M. E. Beckner, et al., Physiol. Behav. 2021, 236, 113413.
- R. Yehuda, S. Brand, R.-K. Yang, Biol. Psychiatry 2006, 59, 660–663.
- 5. G. Cizza, et al., Biol. Psychiatry 2008, 64, 907-911.
- 6. S. D. Mendonsa, M. T. Bowser, J. Am. Chem. Soc. 2005, 127, 9382–9383.

- A. Villalonga, A. M. Pérez-Calabuig, R. Villalonga, Anal. Bioanal. Chem. 2020, 412, 55–72.
- 8. N. K. M. Churcher, S. Upasham, P. Rice, S. Bhadsavle, S. Prasad, *RSC Adv.* **2020**, *10*, 23173–23186.
- N. K. M. Churcher, et al., Biosens. Bioelectron. X 2022, 10, 100145.
- R. E. Fernandez, et al., Electrochem. Commun. 2016, 72, 144– 147
- A. E. Islam, et al., ACS Appl. Nano Mater. 2020, acsanm.0c00353, DOI: .
- H. Richardson, G. Maddocks, K. Peterson, M. Daniele, S. Pavlidis, in 2021 IEEE Sensors, 2021, 1–4, DOI: 10.1109/SENSORS47087.2021.9639832.
- D. Erts, B. Polyakov, H. Olin, E. Tuite, J. Phys. Chem. B. 2003, 107, 3591–3597.
- S. Li, Y. Wang, Z. Zhang, Y. Wang, H. Li, F. Xia, *Anal. Chem.* 2021, DOI: 10.1021/acs.analchem.1c00085.
- R. Levicky, T. M. Herne, M. J. Tarlov, S. K. Satija, J. Am. Chem. Soc. 1998, 120, 9787–9792.
- L. G. Carrascosa, L. Martínez, Y. Huttel, E. Román, L. M. Lechuga, Eur. Biophys. J. 2010, 39, 1433–1444.
- 17. K. Son, T. Uzawa, Y. Ito, T. Kippin, K. W. Plaxco, T. Fujie, *Biochem. Biophys. Res. Commun.* **2023**, 668, 1–7.
- S. Herrwerth, W. Eck, S. Reinhardt, M. Grunze, J. Am. Chem. Soc. 2003, 125, 9359–9366.
- A. Shaver, S. D. Curtis, N. Arroyo-Currás, ACS Appl. Mater. Interfaces 2020, 12, 11214–11223.
- 20. A. Rastogi, et al., Biomacromolecules 2009, 10, pp. 2750-2758.
- H. Richardson, J. Barahona, G. Carter, F. J. Miller, E. Lobaton, S. Pavlidis, in *Hilton Head 2022 Technical Digest*, Hilton Head, SC, USA 2022, 1–4.
- 22. Th. Wink, S. J. van Zuilen, A. Bult, W. P. van Bennekom, *Analyst* **1997**, *122*, 43R–50R.
- 23. M. Yu, et al., J. Phys. Chem. C 2007, 111, 10904-10914.
- 24. I. M. Bhattacharyya, G. Shalev, ACS Sens. 2020, 5, 154-161.
- R. L. Rich, D. G. Myszka, Curr. Opin. Biotechnol. 2000, 11, 54–61.
- 26. A. Tarasov, et al., Biosens. Bioelectron. 2016, 79, 669-678.
- Ó. Gutiérrez-Sanz, N. M. Andoy, M. S. Filipiak, N. Haustein, A. Tarasov, ACS Sens. 2017, DOI: 10.1021/acssensors.7b00187.
- 28. N. Gao, W. Zhou, X. Jiang, G. Hong, T.-M. Fu, C. M. Lieber, *Nano Lett.* **2015**, *15*, 2143–2148.
- S. Dalirirad, A. J. Steckl, Sens. Actuators B Chem. 2019, 283, 79–86.
- 30. B. J. Sanghavi, et al., Biosens. Bioelectron. 2016, 78, 244-252.
- 31. L. López, et al., Anal. Chem. 2021, 93, 973-980.
- 32. J. L. Chávez, K. Rieger, J. A. Hagen, N. Kelley-Loughnane, in *Smart Biomedical and Physiological Sensor Technology XVI*, SPIE, **2019**, pp. 85–91, DOI: 10.1117/12.2520330.
- 33. X. Xu, et al., Nano Lett. 2018, 18, 4130-4135.
- 34. S. Banerjee, et al., Small 2016, 12, 5524-5529.

How to cite this article: H. Richardson, A. Kline, S. Pavlidis, *Electroanalysis* **2024**, *36*, e202300387. https://doi.org/10.1002/elan.202300387

Graphical Abstract

The contents of this page will be used as part of the graphical abstract of html only.

It will not be published as part of main.